Diffusion in Fluids Between Knudsen and Fickian Limits: Departure from Classical Behavior

Gregory L. Aranovich and Marc D. Donohue
Dept. of Chemical & Biomolecular Engineering, The Johns Hopkins University, Baltimore, MD 21218

DOI 10.1002/aic.14926
Published online August 7, 2015 in Wiley Online Library (wileyonlinelibrary.com)

The finite-difference equation of diffusion (consistent with Einstein's evolution equation of diffusion) without the assumption of small mean free path is discussed. This equation predicts significant deviations from classical behavior for the simplest geometry: fluid in a pipe with a large density gradient, such that one end is at the Fickian limit, the other end is at Knudsen limit and there can be a transition zone between them. This has not been considered in previous studies. The analysis indicates that significant deviations from classical (Fickian) behavior arise due to the large change in mean free path which is important in numerous situations, including vacuum technology and propulsion in space. Other examples of deviations from Fick's law include cases where the mean free path is not small compared to system size (nanoscale systems and low density systems) and cases where there are large gradients. These are important in a variety of practical applications, including vacuum distillation, vacuum pumps, and adsorption measurements. © 2015 American Institute of Chemical Engineers *AIChE J*, 61: 3138–3143, 2015
Keywords: diffusion, Einstein's evolution equation, deviations from classical behavior

Introduction

Diffusion in the classical Fickian limit[1] is based on the assumption of small mean free path, λ.[2–5] Rigorously speaking, the Fickian limit requires that $\lambda \to 0$ and this allows fluxes to be defined as being proportional to density gradients.[2] The opposite limit, where the mean free path is much larger than a characteristic size of the system and there are essentially no collisions between particles, is also well known as Knudsen diffusion.[6] In terms of diffusion phenomenology, much less is known about intermediate conditions, where neither Fickian nor Knudsen approaches can be applied. These conditions are fairly common in chemical engineering, including vacuum technology and propulsion systems in space. On the nanoscale, such conditions can arise near solid surfaces and at a gas–liquid interface. The latter is important in any system where there is a phase boundary including adsorption systems and for diffusion in systems with phase transitions.

Previously,[3,7] we considered fluids at these intermediate conditions in the framework of Einstein's evolution equation for diffusion.[8] In publication,[7] we presented an exact solution to Einstein's evolution equation without reducing it to the Fickian approximation, and this solution demonstrated a dramatic difference between Fickian and Einstein's predictions. Einstein's finite-difference equation predicts not only significant quantitative deviations from classical diffusion profiles but also qualitative changes in diffusion mechanisms, such as coexistence of "laminar" and "turbulent" fluxes and "cooperative" transitions between molecular chaos and predominantly ballistic motion of molecules.[7] The reason for the difference between Fickian and Einstein's predictions is that the assumption that $\lambda \to 0$ in the Fickian model turns the original finite-difference equation of mass balance into a differential equation. This can distort density profiles, and, hence, the conditions under which this distortion occurs need to be analyzed.

In this article, we discuss the finite-difference equation of diffusion without the assumption that $\lambda \to 0$ and show that it predicts significant deviations from classical Fickian behavior for the simple case of one-dimensional flow with a large density gradient. In particular, we examine the case of flow where one end is at the Fickian limit, the other end is at Knudsen limit and there can be a large transition zone between them. This has not been considered in previous calculations.

Our goal here is to illustrate (in terms of this simple case) that classical density profiles and fluxes are significantly distorted compared to predictions of Einstein's original finite-difference equation of diffusion. This has fundamental implications for the behavior of fluids between the Knudsen and Fickian limits, and for a variety of practical applications where fluids are at these conditions including low-pressure chemical vapor deposition, various vacuum techniques, and propulsion.

Figure 1 illustrates the classical model of diffusion in a fluid.[2, p. 88] In this model, the number of molecules passing through some surface, S, from left to right is $\frac{1}{6}\bar{V}\rho(x-\lambda,t)$, and the number of molecules passing through this surface from right to left is $\frac{1}{6}\bar{V}\rho(x+\lambda,t)$, where ρ is the local density, that is, the number of molecules per unit of volume. Therefore, the diffusion flux, $F(x, t)$, is

$$F(x,t)=\frac{1}{6}\bar{V}[\rho(x-\lambda,t)-\rho(x+\lambda,t)] \quad (1)$$

Correspondence concerning this article should be addressed to G. L. Aranovich at aranovich@jhu.edu.

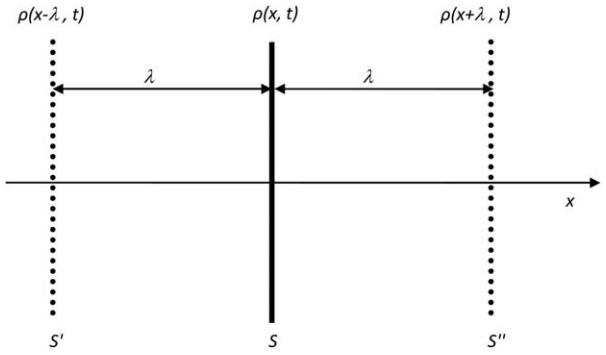

Figure 1. Classical model of diffusion in fluid.

In the classical diffusion model, the finite difference $\rho(x-\lambda, t)-\rho(x+\lambda, t)$ is replaced by the derivative

$$\rho(x-\lambda,t)-\rho(x+\lambda,t) \approx -2\lambda\frac{\partial\rho}{\partial x} \tag{2}$$

and Eq. 1 is changed to $F(x,t)=-\frac{1}{3}\bar{V}\lambda\frac{\partial\rho}{\partial x}$. Plugging this in the mass balance equation

$$\frac{\partial\rho}{\partial t}=-\frac{\partial F}{\partial x} \tag{3}$$

results in the classical diffusion equation

$$\frac{\partial\rho}{\partial t}=\frac{\partial}{\partial x}\left(D\frac{\partial\rho}{\partial x}\right) \tag{4}$$

where

$$D=\frac{1}{3}\bar{V}\lambda \tag{5}$$

The approximation in Eq. 2 assumes that the system is at conditions were there is small λ. However, when conditions are between the Knudsen and Fickian limits, the assumption of small λ is not valid and Eq. 2 cannot be used. Combining Eqs. 1 and 3 results in

$$\frac{\partial\rho(x,t)}{\partial t}=\frac{\partial}{\partial x}\left\{\frac{1}{6}\bar{V}[\rho(x+\lambda,t)-\rho(x-\lambda,t)]\right\} \tag{6}$$

Note that the differential finite-difference Eq. 6 is equivalent to Einstein's evolution equation of diffusion with an exponential distribution free path lengths.[7] Equation 4 (Fick's law) is a particular case of Eq. 6. That is, in the limit of $\lambda \to 0$ the finite-difference Eq. 6 with two independent physical parameters, $\bar{V}$ and λ, turns into a differential Eq. 4 with one independent parameter, $D=\frac{1}{3}\bar{V}\lambda$. Classical models[1] based on the limit of $\lambda \to 0$ are well known. The other limit, where mean-free path is much larger than a characteristic size of the system and there are essentially no collisions between particles, is also well known as Knudsen diffusion.[6] However, to transition between these limits correctly, we need to consider the general finite-difference mass balance in Eq. 6.

Fluid Between Knudsen and Fickian Conditions

Consider a fluid in a pipe when there is a transition from Fickian to Knudsen conditions with $\rho(x)$ being the density distribution along the x axis as shown in Figure 2. In Figure 2, at $x = 0$ there is a small density with $\rho(0) = \rho_0$ and at $x = L$ there is a large density with $\rho(L) = \rho_L$. If ρ_L is large enough (e.g., air at 1atm, or higher) and ρ_0 is small enough (say, vacuum at 10^{-3} atm to 10^{-9} atm), then there is a significant density gradient and the system transitions from Fickian to Knudsen conditions. Such conditions occur in many practical cases, including vacuum technology and jet and rocket propulsion systems.

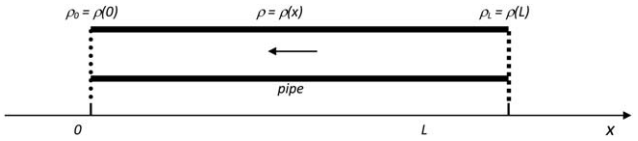

Figure 2. Fluid density, $\rho(x)$, in the pipe changes from $\rho_0 = \rho(0)$ at $x = 0$ to $\rho_L = \rho(L)$ at $x = L$.

The mean-free path of molecules in gases can be estimated from the classical equation[2]

$$\lambda=\frac{1}{\sqrt{2}\pi\sigma^2\rho} \tag{7}$$

where σ is the diameter of molecule. For the system in Figure 2, Eq. 7 indicates that λ can vary from relatively large values (meters) at $x = 0$ to very small values (nanometers) at $x = L$.

Consider a steady-state system with $\frac{\partial\rho}{\partial t}=0$ at all x. For this case, Eqs. 4 and 5 give

$$\frac{\partial}{\partial x}\left(\frac{1}{3}\bar{V}\lambda\frac{\partial\rho}{\partial x}\right)=0 \tag{8}$$

and the differential finite-difference Eq. 6 becomes

$$\frac{\partial}{\partial x}\left\{\frac{1}{6}\bar{V}[\rho(x+\lambda,t)-\rho(x-\lambda,t)]\right\}=0 \tag{9}$$

Fickian Model Based on the Approximation that $\lambda \to 0$

The goal of this article is to show that density profiles and fluxes, predicted by the differential and finite-difference models (Eqs. 8 and 9) are dramatically different for the conditions illustrated in Figure 2. For $\lambda(\rho)$ defined by Eq. 7, Eq. 8 can be solved exactly with boundary conditions

$$\rho(0)=\rho_0 \tag{10}$$

and

$$\rho(L)=\rho_L \tag{11}$$

Taking into account Eq. 7, after first integration, Eq. 8 can be written as

$$\frac{\bar{V}}{3\pi\sqrt{2}\sigma^2\rho}\frac{\partial\rho}{\partial x}=A \tag{12}$$

where A is a constant of integration. Second integration gives from Eq. 12

$$\ln\rho=\frac{3\pi\sqrt{2}\sigma^2}{\bar{V}}Ax+B \tag{13}$$

where B is a constant of the second integration. After imposing boundary conditions (10) and (11), Eq. 13 can be written in the following simple form

$$\frac{\rho(x)}{\rho_0}=\left(\frac{\rho_L}{\rho_0}\right)^{x/L} \tag{14}$$

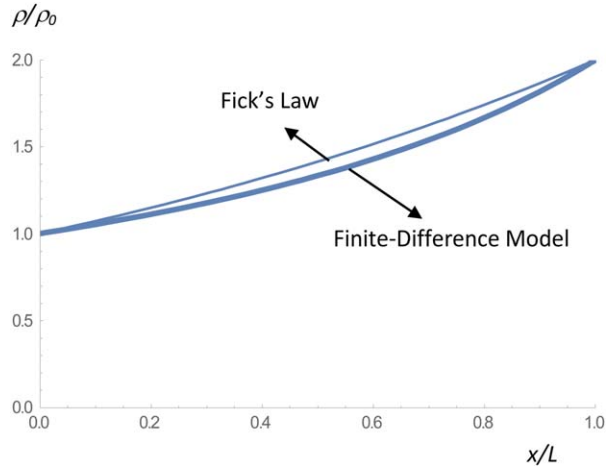

Figure 3. Dependence of ρ/ρ_0 on x/L for $\rho_L/\rho_0 = 2$ predicted by Fick's law Eq. 14 (thin line) and the finite-difference model in Eq. 29 (thick line).

[Color figure can be viewed in the online issue, which is available at wileyonlinelibrary.com.]

Finite Difference Model without the Approximation that $\lambda \to 0$

The steady-state profile for the finite difference model (6) can be analyzed from Eq. 9. Integration of this equation gives

$$\frac{1}{6}\bar{V}[\rho(x+\lambda)-\rho(x-\lambda)]=F \tag{15}$$

or

$$\rho(x+\lambda)-\rho(x-\lambda)=\frac{6F}{\bar{V}} \tag{16}$$

where F is the constant (steady-state) flux through the pipe.

Following the theory of finite-difference equations,[9] consider the general solution of the nonhomogeneous Eq. 16 as a sum of two components: solution of homogeneous equation, ρ_h, and particular solution of the nonhomogeneous equation, ρ_p

$$\rho=\rho_h+\rho_p \tag{17}$$

At $F = 0$, Eq. 16 is homogeneous and its solutions can be representedas a Fourier series[5,10]

$$\rho_h(x)=\sum_{k=0}^{\infty}\left(A_k\cos\frac{k\pi x}{\lambda}+B_k\sin\frac{k\pi x}{\lambda}\right) \tag{18}$$

To analyze the solution of Eq. 16 for $F \neq 0$, assume that the essential contribution to the profile for the system in Figure 2 comes from ρ_p, and ρ_h gives only macroscopically negligible (averaging) oscillations.[10,11] Then

$$\rho(x) \approx \rho_p(x) \tag{19}$$

Consider $\rho_p(x)$ in the form

$$\rho_p(x)=a_x x+b \tag{20}$$

where a_x is a function of x and b is a constant. Plugging ρ_p from Eq. 20 into Eq. 16 gives

$$a_{x+\lambda}(x+\lambda)+b-a_{x-\lambda}(x-\lambda)-b=\frac{6F}{\bar{V}} \tag{21}$$

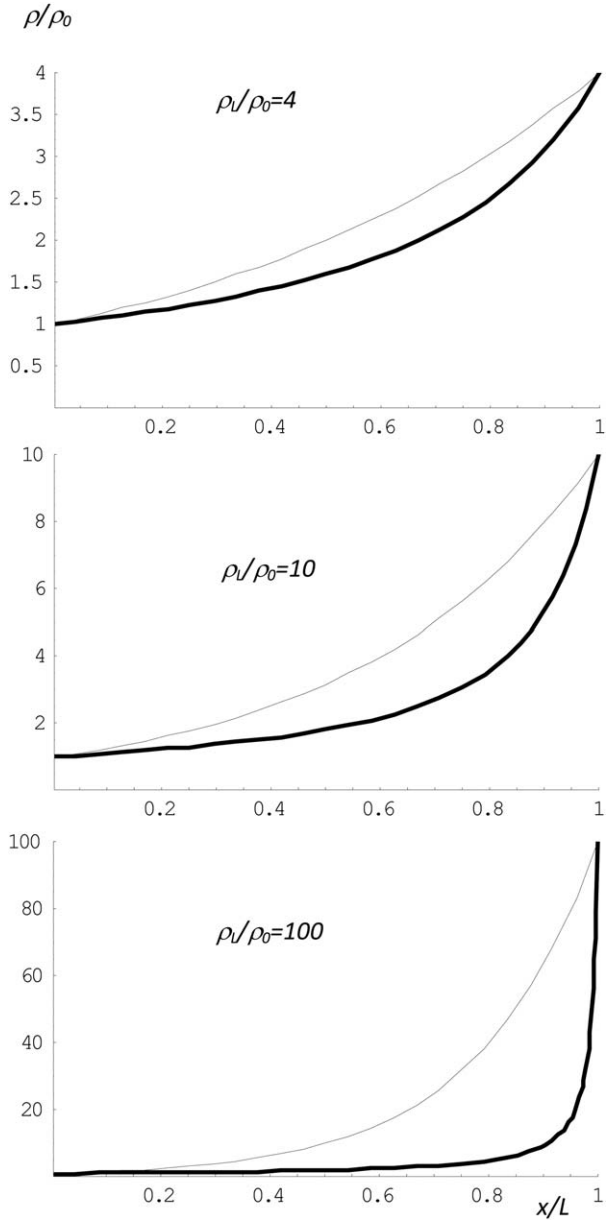

Figure 4. Dependence of ρ/ρ_0 on x/L predicted by Eqs. 14 (thin lines) and 29 (thick lines) for various for ρ_L/ρ_0.

To find the first approximation, consider a_x as a slow function of x, so that

$$a_{x+\lambda} \approx a_{x-\lambda} \tag{22}$$

In this approximation, Eq. 21 gives

$$a_x=\frac{3F}{\bar{V}\lambda} \tag{23}$$

Combining Eqs. 7 and 23 results in

$$a_x=\frac{3\sqrt{2}\pi\sigma^2 F\rho(x)}{\bar{V}} \tag{24}$$

Note that approximation (22) is mathematically compatible with Eq. 24 if ρ does not significantly change between $x+\lambda$ and $x-\lambda$. At the high density end, this is possible due to small λ. At low density end, this is possible if the density gradient is small, and further calculations based on approximation (24)

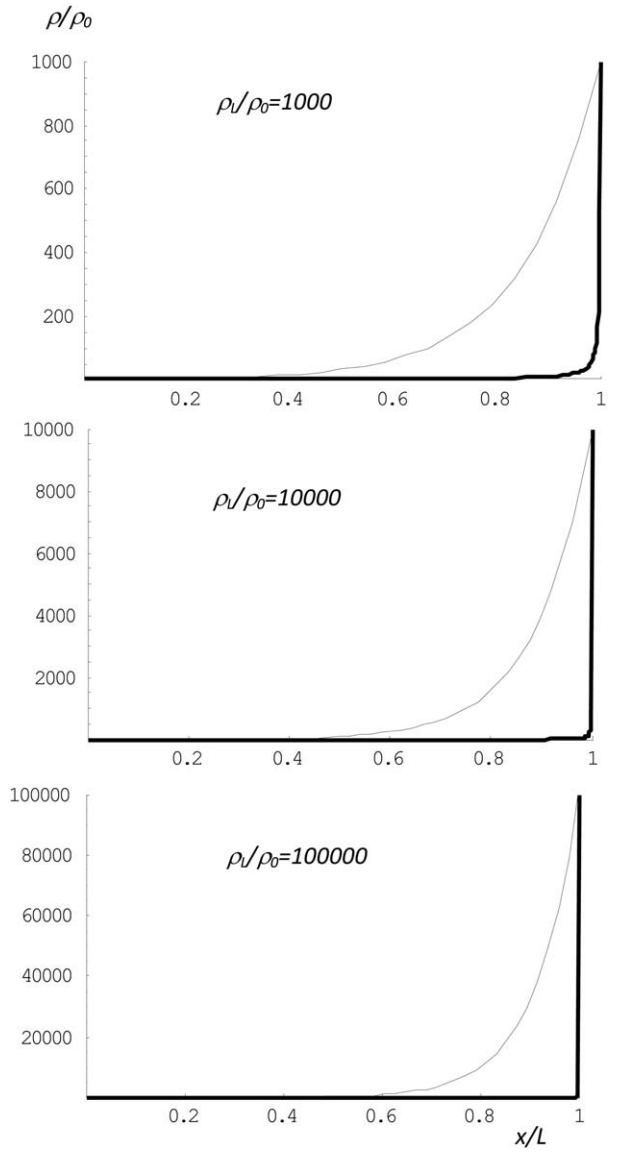

Figure 5. Profiles predicted by Eqs. 14 (thin lines) and 29 (thick lines) for various for ρ_L/ρ_0 between 1000 and 100,000 corresponding to vacuum at one end of the pipe and atmospheric pressure at another end.

(shown in Figures 4 and 5) indicate that this occurs for large ρ_L/ρ_0. In the limit of small ρ_L/ρ_0, $\rho(x)$ becomes slowly changing function, and Eq. 24 is automatically compatible with approximation (22).

Equations 19, 20, and 24 give

$$\rho(x)=\frac{3\sqrt{2}\pi\sigma^2 F}{\bar{V}}x\rho(x)+b \tag{25}$$

Solution of Eq. 25 with respect to $\rho(x)$ results in

$$\rho(x)=\frac{b\bar{V}}{\bar{V}-3\sqrt{2}\pi\sigma^2 Fx} \tag{26}$$

Conditions (10) and (11) give from Eq. 26

$$b=\rho_0 \tag{27}$$

and

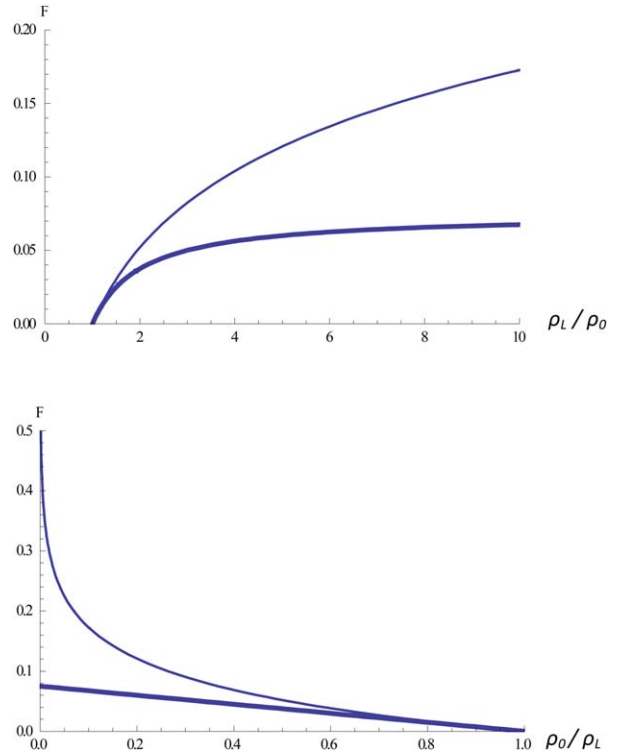

Figure 6. Flux in units of $\frac{\bar{V}}{\sigma^2 L}$ as a function of (a) ρ_L/ρ_0 (upper frame) and (b) ρ_0/ρ_L (lower frame) predicted by Fick's law (Eq. 32; thin line) and finite difference (Eq. 33; thick line).

[Color figure can be viewed in the online issue, which is available at wileyonlinelibrary.com.]

$$\rho(L)=\frac{b\bar{V}}{\bar{V}-3\sqrt{2}\pi\sigma^2 FL} \tag{28}$$

Using Eqs. 27 and 28 to eliminate b and F in Eq. 26 gives

$$\frac{\rho(x)}{\rho_0}=\frac{\rho_L/\rho_0}{\rho_L/\rho_0-(\rho_L/\rho_0-1)x/L} \tag{29}$$

Comparison of Eqs. 14 and 29

In the limit of $\rho_L/\rho_0 \to 1$, both Eqs. 14 and 29 give the same result that $\rho=\rho_0$ everywhere along the length of the pipe. However, when ρ_L/ρ_0 goes up, the difference in predictions between Eqs. 14 and 29 increases. Figure 3 shows the dependence of ρ/ρ_0 on x/L predicted by Eqs. 14 and 29 at $\rho_L/\rho_0 = 2$. As shown in Figure 3, even for $\rho_L/\rho_0 = 2$, the difference in predictions between Eqs. 14 and 29 is apparent.

Figure 4 shows the dependence of ρ/ρ_0 on x/L predicted by Fick's Law Eq. 14 and the finite-difference Eq. 29 for ρ_L/ρ_0 ranging from 4 to 100. As shown in Figure 4, increasing ρ_L/ρ_0 results in significant differences in the predictions between Eqs. 14 and 29, especially in the range of $x/L > 0.2$.

Figure 5 shows profiles predicted by Eqs. 14 and 29 at ratios of ρ_L/ρ_0 between 1000 and 100,000 corresponding to vacuum at one end of the pipe and atmospheric pressure (or higher) at the other end.

As shown in Figure 5, for $x/L > 0.6$, the profiles predicted by Eqs. 14 and 29 are dramatically different for these high ratios of inlet to outlet densities. In particular, the finite-difference Eq. 29 predicts an immediate decrease in density

at the inlet of the pipe with essentially the entire length of the pipe at low density. However, the differential Eq. 14 predicts a more gradual decrease and a low density zone that only is over the last half of the pipe adjacent to the low density end.

Comparison of Fluxes

Since $F=-\frac{1}{3}\bar{V}\lambda\frac{\partial\rho}{\partial x}$, the value of A in Eq. 12 is a steady-state flux through the pipe. Then, with $A=F$, from Eq. 13 it follows that at $x=L$

$$\ln\rho_L=\frac{3\sqrt{2}\pi\sigma^2}{\bar{V}}FL+B \tag{30}$$

and at $x=0$

$$\ln\rho_0=B \tag{31}$$

Combining Eqs. 34 and 35 results in the Fickian flux of

$$F=\frac{\bar{V}}{3\pi\sigma^2L\sqrt{2}}\ln\frac{\rho_L}{\rho_0} \tag{32}$$

Equation 32 gives a steady-state flux calculated from the differential model with approximation (2). Without approximation (2), the steady-state flux for the finite-difference equation can be determined from Eqs. 27 and 28 as follows

$$F=\frac{\bar{V}}{3\pi\sigma^2L\sqrt{2}}\left(1-\frac{\rho_0}{\rho_L}\right) \tag{33}$$

Figure 6 shows fluxes in units of $\frac{\bar{V}}{\sigma^2L}$ predicted by Eqs. 32 and 33 as functions of ρ_L/ρ_0 (upper frame) and as functions of ρ_0/ρ_L (lower frame). For $\bar{V}=500$ m/sec, $\sigma=3.2\times10^{-10}$ m, and $L=1$ m, this unit, $\frac{\bar{V}}{\sigma^2L}$, is about 5×10^{21} molecules/(m^2 s) $\approx10^{-2}$ moles/(m^2 s). As shown in Figure 6, at $\rho_L>2\,\rho_0$ the finite-difference model, Eq. 33, predicts significantly smaller fluxes than Fick's law, Eq. 32.

The Fick's law flux (Eq. 32) predicts that F increases to infinity as ρ_0 goes to zero. This is both incorrect and unphysical. In the finite difference model of Eq. 33 this problem is resolved and it gives a finite limit for the flux through the pipe at $\rho_0\to0$

$$\lim_{\rho_0\to0}F=\frac{\bar{V}}{3\pi\sigma^2L\sqrt{2}} \tag{34}$$

This result is especially important for the analysis of propulsion systems in space.

Note that here we considered only one example of conditions where Fick's law fails due to a large change in mean free path. This is important for various applications, such as vacuum techniques and propulsion in space. Other examples include cases where mean free path is not small compared to system size (nanoscale, low density) and cases where there are large gradients. In these cases, the mass balance needs to be considered in terms of the differential finite-difference Eq. 6.

Relevance to Chemical Engineering Applications and Discussion

Diffusion of fluids is widely used in chemical engineering.[12–15] Numerous applications include agitation, ducts, fluidization, vacuum techniques, pumps, adsorption measurements, and various related fields (see e.g., Chapters 9–13 in Ref. 13). For many applications, approximation (2) is valid and Fick's law is applicable. However, there are situations, such as vacuum technology and propulsion in space, where fluid moves from relatively high density to near vacuum. This can occur in vacuum pumps, in microelectronics technology chambers, in thermostats (leaks to vacuum compartments), in vacuum distillation columns, and in many other cases where fluid density can significantly change (such as rate-limiting processes for the sublimation of small molecule organic semiconductors[16]). In such cases, approximation (2) is not correct and more general Eq. 6 should be considered.

To illustrate the relevance of our model to chemical engineering applications, consider a situation where one needs to fill a cylinder with oxygen. If this cylinder contains air, it needs to be pumped out to a certain vacuum (say, 10^{-3} atm). The next step is filling of the tank with oxygen from a source (say, from a tank with oxygen) into the evacuated cylinder through a pipe (as shown in Figure 2). Such situations are ubiquitous in chemical engineering and their understanding on a fundamental level is essential. Certainly, transport of gas through pipes is a complex phenomenon, and here (to illustrate a fundamental problem) we considered one of the simplest cases.

A more general treatment could include anisotropy in both the mean free path and the average molecular velocity[17] (i.e., temperature gradient). If V_+ and V_- are average velocities in the + and − directions and λ_+ and λ_- are mean free paths in the + and − directions, then the net flux is represented as $F=V_+\rho_+-V_-\rho_-$ where ρ_+ and ρ_- are densities at points $x+\lambda_+$ and $x-\lambda_-$. Therefore

$$F=(V\rho)|_{x-\lambda_-}-(V\rho)|_{x+\lambda_+} \tag{35}$$

and

$$F=V_-\rho_--V_+\rho_+\equiv\frac{V_++V_-}{2}(\rho_--\rho_+)+\frac{\rho_++\rho_-}{2}(V_--V_+) \tag{36}$$

Hence, the net flux can be written as the sum of a convection (flow) term, F_c, and a diffusion term, F_d, as

$$F=F_c+F_d \tag{37}$$

where

$$F_c=\frac{\rho_++\rho_-}{2}(V_--V_+) \tag{38}$$

and

$$F_d=\frac{V_++V_-}{2}(\rho_--\rho_+) \tag{39}$$

If $V_+=V_-$, $\lambda_+=\lambda_-$, $\rho_-=(1/6)\rho(x-\lambda,\,t)$, and $\rho_+=(1/6)\rho(x+\lambda,\,t)$, then $F_c=0$ and F_d coincides with $F(x,\,t)$ in Eq. 1.

However, plugging Eqs. 37–39 into Eq. 3 gives

$$\frac{\partial\rho}{\partial t}=V_M\frac{\partial\bar{\rho}}{\partial x}+\bar{V}\frac{\partial(\rho_+-\rho_-)}{\partial x} \tag{40}$$

where V_M is the (net) macroscopic velocity

$$V_M=V_--V_+ \tag{41}$$

$\bar{V}$ is the average molecular velocity

$$\bar{V}=\frac{V_++V_-}{2} \tag{42}$$

and $\bar{\rho}$ is the average density

$$\bar{\rho} = \frac{\rho_+ + \rho_-}{2} \tag{43}$$

Note that Eqs. 40–43 imply that V_M and $\bar{V}$ are constant. Further, if $\rho_+ - \rho_- \approx \delta \frac{\partial \rho}{\partial x}$ and $\bar{\rho} = \rho$, then Eq. 40 can be written in the following form

$$\frac{\partial \rho}{\partial t} = V_M \frac{\partial \rho}{\partial x} + D \frac{\partial^2 \rho}{\partial x^2} \tag{44}$$

where $D = \bar{V}\delta$, and δ is a distance where ρ changes from ρ_+ to ρ_-. This is the conventional mass balance equation found in most text on fluid mechanics. However, this derivation shows explicitly that Eq. 44 is based on the assumptions that V_M and $\bar{V}$ are constant and that $\rho_+ - \rho_- \approx \delta \frac{\partial \rho}{\partial x}$. Since δ is proportional to the mean free path, λ, the latter assumption is limited by small λ and small density gradients. Hence, the conventional concept of the mass balance takes the fluxes in Eq. 35 and breaks them into convection (flow) and diffusion terms in a way that is valid in some situations but is not universal.

Note that approximation (2) reduces the nonlocal (finite-difference) Eq. 6 to a local differential Eq. 4. Equation 6 includes direct special correlations for points separated by 2λ. In a real fluid with finite λ, collisions of molecules are not randomly distributed in space, but correlated. In other words, Fick's law is consistent with Markovian random process though real fluids are non-Markovian.[18] The nature of such correlations has been discussed in literature, in particular in,[19–26] and there have been attempts[18] to modify Fick's law to take into account non-Markovian (memory) effects. As we have shown here, this can be done by using finite difference model without approximation (2).

Literature Cited

1. Fick A. Ueber Diffusion (in German). *Phil Mag*. 1855;10:30–39.
2. Boltzmann L. Zur Integration der Diffusionsgleichung bei variabeln Diffusionscoefficienten (in German). *Ann Phys*. 1894;289:959–964.
3. Aranovich GL, Donohue MD. Limitations and Generalizations of the Classical Phenomenological Model for Diffusion in Fluids. *Mol Phys*. 2007;105:1085–1093.
4. Aranovich GL, Donohue MD, Eliminating the Mean-Free-Path Inconsistency in Classical Phenomenological Model of Diffusion for Fluids. *Phys A*. 2007;373:119–141.
5. Aranovich GL, Donohue MD. Diffusion in Fluids with Large Mean Free Paths: Non-classical Behavior between Knudsen and Fickian Limits. *Phys A*. 2009;388:3355–3370.
6. Knudsen M. *The Kinetic Theory of Gases*. London: Methuen & Co. Ltd., 1950.
7. Aranovich GL, Donohue MD. Exact solution to Einstein's evolution equation for fluid with exponential free paths distribution. In: Claes A, editor. *Evolution Equations*, Chapter 4. Nova Science Publishers, New York, 2011.
8. Einstein A. *Ann Phys*. 1905;322:549–560 (English translation: *Investigations on the Theory of the Brownian Movement*. New York: Dover, 1956).
9. Gelfond AO. *Calculus of Finite Differences*. Moscow: Nauka, 1967.
10. Aranovich GL, Donohue MD. Resolving the Inconsistency between Classical Diffusion and Adsorption. *Langmuir*. 2009;25:3577–3583.
11. Nicholson D, Parsonage NG. *Computer Simulation and the Statistical Mechanics of Adsorption*. London: Academic Press, 1982.
12. Bird RB, Stewart WE, Lightfoot EN. *Transport Phenomena*, *2nd ed.* New York: Wiley, 2000.
13. Cussler EL. *Diffusion, Mass Transfer in Fluid Systems*, *2nd ed.* Cambridge: University Press, 1997.
14. Brodkey RS, Hershey HC. *Transport Phenomena. Chemical Engineering Series*. Boston: McGraw-Hill, 1988.
15. Hines AL, Maddox RN. *Mass Transfer: Fundamentals and Applications*. Englewood Cliffs, New Jersey: Prentice Hall, 1985.
16. Morgan NT, Zhang Y, Molitor EJ, Bell BM, Holmes RJ, Cussler EL. Understanding rate-limiting processes for the sublimation of small molecule organic semiconductors. *AIChE J*. 2014;60:1347–1354.
17. Aranovich GL, Whitman JR, Donohue MD. Modification of Classical Approximations for Diffusion in Fluids with Density Gradients. *Phys Chem Chem Phys*. 2010;12:9043–9052.
18. Alley WE, Alder BJ. Modification of Fick's law. *Phys Rev Lett*. 1979;43:653–656.
19. Alder BJ, Alley WE. Long-time correlation effects on displacement distributions. *J Stat Phys*. 1978;19:341–347.
20. Alder BJ. Slow dynamics by molecular dynamics. *Phys A*. 2002;315:1–4.
21. Bakunin O. *Turbulence and Diffusion*. Berlin: Springer-Verlag, 2008.
22. Robles-Dominguez JA, Silva B, Garsia-Colin LS. Non-linear constitutive and diffusion equations in the Burnett regime. *Phys A*. 1981;106:539–558.
23. McLennan JA. Onsager's Theorem and Higher-order Hydrodynamic Equations. *Phys Rev A*. 1974;10:1272.
24. McLennan JA. Burnett Coefficients and Correlation Functions. *Phys Rev A*. 1973;8:1479.
25. Grmela M. Onsager's Symmetry in Higher Order Fluid Dynamics. *Helv Phys Acta*. 1977;50:393.
26. de Schepper IM, Ernst MH. Self-Diffusion beyond Fick's Law. *Phys A*. 1979;98:189.

Manuscript received Feb. 6, 2015, and revision received June 5, 2015.